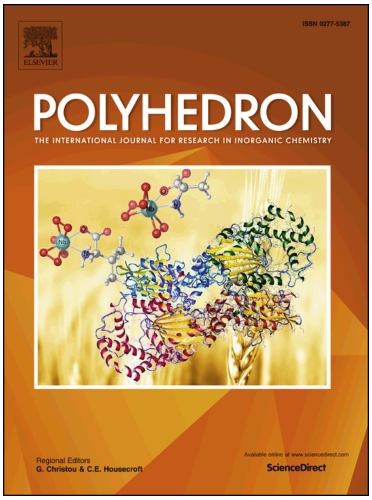

Transesterification reactions of dimethoxycarbonylethyltin- morpholinodithiocarbamate, [$(MeO_2CCH_2CH_2)_2Sn(MDTC)_2$]: Synthesis, spectroscopy, X-ray structural characterization and DFT calculations of new diestertin dithiocarbamate complexes - Part II

B.P. de Morais, C.L. Donnici, B.L. Rodrigues, G.M. de Lima, J.L. Wardell, M.A.C. Nascimento, R.S. Bitzer

PII: S0277-5387(17)30464-3
DOI: http://dx.doi.org/10.1016/j.poly.2017.06.046
Reference: POLY 12727

To appear in: *Polyhedron*

Received Date: 10 April 2017
Accepted Date: 28 June 2017

Please cite this article as: B.P. de Morais, C.L. Donnici, B.L. Rodrigues, G.M. de Lima, J.L. Wardell, M.A.C. Nascimento, R.S. Bitzer, Transesterification reactions of dimethoxycarbonylethyltin- morpholinodithiocarbamate, [$(MeO_2CCH_2CH_2)_2Sn(MDTC)_2$]: Synthesis, spectroscopy, X-ray structural characterization and DFT calculations of new diestertin dithiocarbamate complexes - Part II, *Polyhedron* (2017), doi: http://dx.doi.org/10.1016/j.poly.2017.06.046

Transesterification reactions of dimethoxycarbonylethyltin-morpholinodithiocarbamate, [$(MeO_2CCH_2CH_2)_2Sn(MDTC)_2$]: Synthesis, spectroscopy, X-ray structural characterization and DFT calculations of new diestertin dithiocarbamate complexes - Part II

B.P. de Morais [a], C.L. Donnici [a], B.L. Rodrigues [a], G.M. de Lima [a,*],
J.L. Wardell [b, c], M.A.C. Nascimento [d], and R.S. Bitzer [d,*]

[a] *Departamento de Química, Universidade Federal de Minas Gerais, UFMG, Avenida Antônio Carlos 6627, Belo Horizonte, MG, 31270-901, Brazil*

[b] *Fiocruz - Fundação Oswaldo Cruz, Instituto de Tecnologia em Fármacos, Farmanguinhos, Rio de Janeiro, RJ, 21041-250, Brazil*

[c] *Department of Chemistry, University of Aberdeen, Old Aberdeen, AB24 3UE, Scotland, UK*

[d] *Instituto de Química, Universidade Federal do Rio de Janeiro, UFRJ, Rio de Janeiro, RJ, 21941-909, Brazil*

Abstract

The scarcity of studies concerning diestertin(IV) dithiocarbamate complexes led us to investigate the spectroscopic and structural properties of [$(RO_2CCH_2CH_2)_2Sn(MDTC)_2$] (R = Me (**1**) or Et (**2**); MDTC = morpholinodithiocarbamate). The reaction of [$(MeO_2CCH_2CH_2)_2SnCl_2$] with sodium morpholinodithiocarbamate (NaMDTC) in $CHCl_3$ afforded (**1**), while the transesterification reaction of (**1**) with EtOH in the presence of dmso yielded (**2**). Both diestertin(IV) complexes were characterized by elemental analysis, FTIR and multinuclear (^1H, ^{13}C and ^{119}Sn) NMR spectroscopy, and single-crystal X-ray diffraction. Our X-ray structural analysis revealed that (**1**) and (**2**) exhibit a distorted pentagonal bipyramidal coordination geometry. In both cases, the apical positions are occupied by ester groups while the equatorial plane displays two bidentate morpholinodithiocarbamate ligands and one intramolecular C=O···Sn interaction. The O···Sn distances amount to 2.632 (**1**) and 2.618 Å (**2**). According to our supramolecular analysis, the crystal arrangement of each product is assembled by weak C-H···O and C-H···S hydrogen bonds. Finally, a DFT study of the six- and seven-coordinate forms of (**1**) and (**2**) allowed an upper-bound estimate of the intramolecular C=O···Sn interaction energy, -3.7 kcal mol^{-1}.

Keywords: Organotin dithiocarbamate; Estertin; Structural determination; Weak hydrogen bond; DFT calculations.

---

* Corresponding authors: gmlima@ufmg.br (Prof. G.M. de Lima) and rodrigobitzer@gmail.com (Dr. R.S. Bitzer).

1. Introduction

In the middle of the 19th century, Sir Edward Frankland reported the synthesis of diethyltin diiodide, giving rise to organotin chemistry [1,2]. After the discovery of Grignard reagents, organotin chemistry evolved a great deal, consolidating itself as one of the most prolific subareas of organometallic chemistry [3]. Nevertheless, biological and industrial applications of organotin compounds only started to emerge a century after Frankland's seminal work [3-6]. Specifically, estertin(IV) compounds were introduced by AKZO Chemie in the mid-1970s as more efficient and less toxic PVC stabilizers [7-9].

Monoestertin(IV) derivatives have received much attention in the literature. They display a variety of coordination geometries due to the possibility of intramolecular $C=O\cdots Sn$ interaction, as confirmed by X-ray structure analyses and theoretical calculations [10-22]. Furthermore, monoestertin(IV) compounds readily undergo transesterification reactions owing to the increased electrophilicity of the carbonyl group semi-coordinated to tin [23-27].

Unlike monoestertins, examples of diestertin(IV) compounds are relatively limited [11,16,28-38]. Under basic conditions, $[(MeO_2CCH_2CH_2)_2SnCl_2]$ eliminates MeOH yielding di(carboxylethyl)tin, $C_6H_8O_4Sn$, which can be converted into $[(RO_2CCH_2CH_2)_2SnCl_2]$ upon dissolution in alcoholic HCl solutions [28]. In addition, $[(MeO_2CCH_2CH_2)_2SnCl_2]$ can undergo salt metathesis reactions affording new bis(2-methoxycarbonylethyl)tin(IV) derivatives [30,31,37,38]. Diestertin(IV) compounds can also go through transesterification reactions [32,38]. In 2007, Dong reported the preparation of $[(EtO_2CCH_2CH_2)_2SnCl_2]$ by reaction of $[(MeO_2CCH_2CH_2)_2SnCl_2]$ with EtOH [32]. Recently, we have shown that a series of diestertin(IV) dithiocarbamate complexes can be easily obtained by transesterification reactions in the presence of dmso [38].

As part of our ongoing interest in organotin chemistry [15,33,38-50], we have undertaken a project aiming to elucidate spectroscopic and structural properties of diestertin(IV) dithiocarbamate complexes [38]. Previous studies on these compounds deal with seven-coordinated $[(MeO_2CCH_2CH_2)_2Sn(S_2CNR_2)_2]$ (R = Me or Et) [37,51] and $[(MeO_2CCH_2CH_2)_2SnCl(S_2CNMe_2)]$, which adopts a distorted trigonal bipyramidal coordination geometry [52]. In addition, we have recently described the spectroscopic and structural properties of $[(RO_2CCH_2CH_2)_2Sn(PDTC)_2]$ (R = Me, Et, Pr or Bu; PDTC = pyrrolidinodithiocarbamate), in which the geometry at the metal centres is a distorted pentagonal bipyramid [38]. In this article, we report the synthesis, spectroscopy, X-ray structure and Hirshfeld surface analyses, and DFT study of $[(RO_2CCH_2CH_2)_2Sn(MDTC)_2]$ (R

= Me (**1**) or Et (**2**); MDTC = morpholinodithiocarbamate), extending our earlier work on the subject [38]. This article shows that (**1**) and (**2**) also exhibit seven-coordinate Sn(IV) centres due to intramolecular C=O···Sn interactions. Moreover, a DFT study of the six- and seven-coordinate forms of (**1**) and (**2**) has allowed an estimate of the C=O···Sn interaction energy.

2. Computational and experimental details

2.1. Materials and instruments

Starting materials and reagent grade solvents were purchased from Aldrich, Alfa-Aesar, Fluka, Merck, Synth or Vetec and used as received. The organotin(IV) precursor [$(MeO_2CCH_2CH_2)_2SnCl_2$] was prepared according to the literature [11,53], and NaMDTC was obtained from morpholine, CS_2 and NaOH. ^1H and $^{13}C\{^1H\}$ NMR spectra in solution were recorded at 200 and 50 MHz, respectively, using a Bruker DPX-200 spectrometer equipped with an 89 mm wide-bore magnet. The $^{13}C\{^1H\}$ NMR spectra of (**1**) and (**2**) are shown in Figure S1 (Appendix A). $^{119}Sn\{^1H\}$ NMR spectra were recorded at 400 MHz using a Bruker Advance III DPX-400 spectrometer equipped with an 89 mm wide-bore magnet. The $^{119}Sn\{^1H\}$ NMR spectra of (**1**) and (**2**) are depicted in Figure S2 (Appendix A). ^1H and $^{13}C\{^1H\}$ chemical shift (δ/ppm) values were determined relative to $SiMe_4$, and the $^{119}Sn\{^1H\}$ δ values were determined relative to $SnMe_4$. The FTIR spectra were recorded using KBr pellets on a PerkinElmer 238 FTIR spectrometer. C, H and N microanalyses were performed on a PerkinElmer PE-2400 CHN analyser. Single-crystal X-ray diffraction data were acquired at 150(1) K using a Xcalibur Atlas Gemini ultra-diffractometer and graphite-monochromated Mo-Kα radiation (λ = 0.71073 Å). Data collection, reduction and cell refinement were performed with CrysAlisPro [54]. The crystal structures were solved by Direct Methods using SHELXS-97 [55] and refined by full-matrix least squares on F^2 using SHELXL-2014 [56]. All H atoms were geometrically positioned and refined as riding on their respective C atoms. WinGX was used as graphical interface for structure solution and refinement [57]. The crystal structures were analysed with Mercury [58] and PLATON [59]. Material for publication, including CIFs and molecular graphics, was prepared using Mercury [58] and enCIFer [60]. Crystal data and structure refinement parameters for (**1**) and (**2**) are summarized in Table I.

Insert Table I

Molecular Hirshfeld surfaces have been constructed from CIFs in order to dissect crystal structures into noncovalent contacts [62-65]. The very high-resolution Hirshfeld surfaces for (**1**) and (**2**) were generated by CrystalExplorer 3.1 [66], and functions of curvature and distance, including shape index and d_{norm}, were mapped onto the surfaces. In addition, two-dimensional fingerprint (d_i,d_e) plots were used to illustrate individual intermolecular contributions to the crystal structures (Figures S3 and S4, Appendix A).

*2.2. Synthesis of $[(MeO_2CCH_2CH_2)_2Sn(MDTC)_2]$ (**1**)*

$[(MeO_2CCH_2CH_2)_2SnCl_2]$ (0.983 g, 2.70 mmol) dissolved in $CHCl_3$ (10 mL) was slowly added to a suspension of NaMDTC (1.10 g, 5.94 mmol) in the same solvent (20 mL). After 24 h reflux, the solvent was pumped off and the remaining oily residue was washed with Et_2O, affording a white precipitate, which was recrystallized from a mixture of $MeOH:CH_2Cl_2$:dmso (50:50:1). X-ray quality single crystals were grown as the solvent mixture cooled to room temperature. Yield: 65% (0.872 g, 1.41 mmol). M.p.: 141-143°C. *Anal.* Calc. for $C_{18}H_{30}N_2O_6S_4Sn$ (FW 617.37): C, 35.02; H, 4.90; N, 4.74%. Found: C, 35.08; H, 4.58; N, 4.71%. FTIR (KBr, ν_{max}/cm^{-1}): 1740/1709 ν(CO); 1464 ν(CN); 1005 ν(CS); 560/547 ν(Sn-C). ^{1}H NMR ($CDCl_3$, δ/ppm): 4.05-4.03 {m, 4H, $S_2CN(CH_2C\underline{\mathbf{H}}_2)_2O$}, 3.71-3.69 {m, 4H, $S_2CN(C\underline{\mathbf{H}}_2CH_2)_2O$}, 3.67 {s, 6H, $Sn(CH_2CH_2CO_2C\underline{\mathbf{H}}_3)_2$}, 2.97 {t, 4H, $Sn(CH_2C\underline{\mathbf{H}}_2CO_2Me)_2$, $^3J_{H-H}$ = 8.1 Hz, $^3J_{Sn-H}$ = 113.6 Hz}, 2.25 {t, 4H, $Sn(C\underline{\mathbf{H}}_2CH_2CO_2Me)_2$, $^3J_{H-H}$ = 8.1 Hz; $^2J_{Sn-H}$ = 92.9 Hz}. ^{13}C NMR ($CDCl_3$, δ/ppm): 202.1 {$S_2\underline{\mathbf{C}}N(CH_2CH_2)_2O$}, 176.5 {$Sn(CH_2CH_2\underline{\mathbf{C}}O_2Me)_2$, $^3J_{Sn-C}$ = 127.9 Hz}, 66.1 {$S_2CN(CH_2\underline{\mathbf{C}}H_2)_2O$}, 51.2 {$S_2CN(\underline{\mathbf{C}}H_2CH_2)_2O$}, 52.2 {$Sn(CH_2CH_2CO_2\underline{\mathbf{C}}H_3)_2$}, 32.8 {$Sn(\underline{\mathbf{C}}H_2CH_2CO_2Me)_2$, $^1J_{Sn-C}$ = 804.8/768.9 Hz}, 30.8 {$Sn(CH_2\underline{\mathbf{C}}H_2CO_2Me)_2$, $^2J_{Sn-C}$ = 40.1 Hz}. ^{119}Sn NMR ($CDCl_3$, δ/ppm): -436.7 {$^1J_{Sn-C}$ = 804.3 Hz, $^3J_{Sn-C}$ = 130.3 Hz}.

*2.3. Synthesis of $[(EtO_2CCH_2CH_2)_2Sn(MDTC)_2]$ (**2**)*

A round bottom flask (50 mL) was charged with (**1**) (0.881 g, 1.43 mmol) and a mixture of EtOH (15 mL) and dmso (0.30 mL). After 30 min reflux, the resulting solution was left standing at room temperature. X-ray quality crystals were obtained after 24 h. Yield: 61% (0.563 g, 0.872 mmol). M.p.: 93-94°C. *Anal.* Calc. for $C_{20}H_{34}N_2O_6S_4Sn$ (FW 645.42): C, 37.22; H, 5.31; N, 4.34%. Found: C, 37.32; H, 5.21; N, 4.40%. FTIR (KBr, ν_{max}/cm^{-1}): 1731/1694 ν(CO); 1463 ν(CN); 1000 ν(CS); 562/543 ν(Sn-C). ^{1}H NMR ($CDCl_3$, δ/ppm):

4.12-4.05 {m, 4H, $Sn(CH_2CH_2CO_2C\underline{\boldsymbol{H}}_2CH_3)_2$}, 3.98 {m, 4H, $S_2CN(CH_2C\underline{\boldsymbol{H}}_2)_2O$}, 3.63 {m, 4H, $S_2CN(C\underline{\boldsymbol{H}}_2CH_2)_2O$}, 2.88 {t, 4H, $Sn(CH_2C\underline{\boldsymbol{H}}_2CO_2Et)_2$, $^3J_{H\text{-}H} = 8.0$ Hz; $^3J_{Sn\text{-}H} = 114.4$ Hz}, 2.16 {t, 4H, $Sn(C\underline{\boldsymbol{H}}_2CH_2CO_2Et)_2$, $^3J_{H\text{-}H} = 7.9$ Hz, $^2J_{Sn\text{-}H} = 93.8$ Hz}, 1.16 {t, 6H, $Sn(CH_2CH_2CO_2CH_2C\underline{\boldsymbol{H}}_3)_2$, $^3J_{H\text{-}H} = 7.0$ Hz}. ^{13}C NMR ($CDCl_3$, δ/ppm): 202.1 {$S_2\underline{\boldsymbol{C}}N(CH_2CH_2)_2O$}, 175.9 {$Sn(CH_2CH_2\underline{\boldsymbol{C}}O_2Et)_2$, $^3J_{Sn\text{-}C} = 127.7$ Hz}, 65.9 {$S_2CN(CH_2\underline{\boldsymbol{C}}H_2)_2O$}, 60.9 {$Sn(CH_2CH_2CO_2\underline{\boldsymbol{C}}H_2CH_3)_2$}, 51.0 {$S_2CN(\underline{\boldsymbol{C}}H_2CH_2)_2O$}, 32.8 {$Sn(\underline{\boldsymbol{C}}H_2CH_2CO_2Et)_2$}, 30.8 {$Sn(CH_2\underline{\boldsymbol{C}}H_2CO_2Et)_2$, $^2J_{Sn\text{-}C} = 42.8$ Hz}, 14.1 {$Sn(CH_2CH_2CO_2CH_2\underline{\boldsymbol{C}}H_3)_2$}. ^{119}Sn NMR ($CDCl_3$, δ/ppm): -443.2 {$^1J_{Sn\text{-}C} = 812.6$ Hz; $^3J_{Sn\text{-}C} =$ 123.1 Hz}.

2.4. DFT calculations

All calculations were carried out with JAGUAR 7.9 [67] using an energy convergence criterion of 1.00 x 10^{-8} hartree. Gas-phase geometry optimizations were performed without constraints using the B3LYP [68] hybrid functional along with the LACV3P** basis set. The crystal structures of (**1**) and (**2**) were used as input geometries. Relative total energies (ΔE_T/kcal mol^{-1}) of the six- and seven-coordinate forms of both products were calculated as follows: $\Delta E_T = E^{(six)} - E^{(seven)} = \Delta E_{SCF} + \Delta E_{ZPE}$, in which E_{SCF} is the SCF total energy and E_{ZPE} is the zero point energy. The vibrational frequencies of the optimized geometries were computed at the same level of calculation from analytic second derivatives and verified to be real. They were used in support of our FTIR band assignments. Gas-phase thermodynamic properties were evaluated at 298.15 K and 1.00 atm.

3. Results and discussion

3.1. Synthesis and preliminary characterization

Product (**1**) was prepared by salt metathesis from $[(MeO_2CCH_2CH_2)_2SnCl_2]$ and NaMDTC, while (**2**) was synthesized by transesterification reaction of (**1**) with EtOH in the presence of dmso (Scheme 1). Both diestertin(IV) compounds were obtained in moderate yields as analytically pure colourless solids, as confirmed by satisfactory melting ranges and elemental analyses.

Insert Scheme 1

The FTIR spectra of (**1**) and (**2**) exhibit two bands assigned to *ν*(CO), namely 1740 and 1709 cm^{-1} (**1**) and 1731 and 1694 cm^{-1} (**2**). The *ν*(CO) bands at lower wavenumbers (1709 and 1694 cm^{-1}) are ascribed to the semi-coordinated C=O groups of (**1**) and (**2**). These values fall within the expected range for diestertin(IV) dithiocarbamate complexes [38]. In the starting diestertin compound, $[(MeO_2CCH_2CH_2)_2SnCl_2]$, only one *ν*(CO) band is seen at 1677 cm^{-1}. For both (**1**) and (**2**), vibrations related to the dithiocarbamate backbone occur in the typical regions [38]. Moreover, each product exhibits two *ν*(Sn-C) bands in the range 600-500 cm^{-1}.

3.2. Multinuclear NMR

Insert Scheme 2

The NMR signals for (**1**) and (**2**) lie in the expected regions (Figures S1 and S2, Appendix A) [38,69]. The ^{1}H NMR signals for the ester groups of (**1**) and (**2**) are not too different from those observed for $[(MeO_2CCH_2CH_2)_2SnCl_2]$. The $^3J(^{119/117}Sn-^1H)$ values [H5, H5`: 113.6 (**1**) and 114.4 Hz (**2**)] are systematically greater than the corresponding $^2J$ parameters [H4, H4`: 92.9 (**1**) and 93.9 Hz (**2**)]. Stereo-electronic effects, such as geometry and electronegativity of the ligands, might affect the magnitude of $^nJ(^{119/117}Sn-^1H)$.

Only one set of signals for the morpholine group was observed in the ^{13}C NMR spectra of (**1**) and (**2**). The signal for the NCS_2 moiety observed at δ 202.1 stands out among the other chemical shifts for the dithiocarbamate fragment [69]. Recently, we have detected two ^{13}C resonances for the carbonyl groups of $[(EtO_2CCH_2CH_2)_2Sn(PDTC)_2]$ and $[(BuO_2CCH_2CH_2)_2Sn(PDTC)_2]$ (PDTC = pyrrolidinedithiocarbamate) assigned to free and semi-coordinated ^{13}C=O [38]. The morpholine analogues (**1**) and (**2**) display only one ^{13}C signal detected at δ 176 [$^2J(^{119/117}Sn-^{13}C)$, 126 (**1**) and 182 Hz (**2**)], as also observed for $[(MeO_2CCH_2CH_2)_2Sn(PDTC)_2]$ and $[(PrO_2CCH_2CH_2)_2Sn(PDTC)_2]$ [38]. It is possible that an exchange between hexa and heptacoordinated forms in solution averages the ^{1}H and ^{13}C NMR signals, preventing detectable differences between the ester groups of (**1**) and (**2**). The signals for C4 and C5, near δ 30, could not be distinguished from those observed for C4` and C5` in the ^{13}C NMR spectra of the products. The $^1J(^{119}Sn-^{13}C)$ values for C4/C4`, 804.3 (**1**) and 812.6 Hz (**2**), are larger than the respective constant for $[(MeO_2CCH_2CH_2)_2SnCl_2]$ (792 Hz).

In the $^{119}Sn\{^1H\}$ NMR spectra of (**1**) and (**2**), signals appear at δ -436.7 [$^1J(^{119}Sn-^{13}C)$ = 804.3 Hz, $^3J(^{119}Sn-^{13}C)$ = 130.3 Hz] and δ -443.2 [$^1J(^{119}Sn-^{13}C)$ = 812.6 Hz, $^3J(^{119}Sn-^{13}C)$ =

123.1 Hz], respectively. In several studies reported in the literature the C-Sn-C angles (θ) obtained from the $^{1}J(^{119}Sn-^{13}C)$ coupling constants are compared with those values provided by X-ray crystallography [70]. This information is valuable in determining similarities between solution- and solid-state structures. In this work, the C-Sn-C angles (θ) in solution, 155.2° (**1**) and 156.0° (**2**), were evaluated using the following empirical equations:

$|^{1}J(^{119}Sn-^{13}C)| = 11.4\ \theta - 875$ for Me-Sn-Me (1),

$|^{1}J(^{119}Sn-^{13}C)| = [(9.99\pm0.73)\ \theta - (746\pm100)]$ for Bu-Sn-Bu (2),

$|^{1}J(^{119}Sn-^{13}C)| = [(15.56\pm0.84)\ \theta - (1160\pm101)]$ for Ph-Sn-Ph (3).

The average θ values obtained by single-crystal X-ray diffraction experiments (Section 3.3), 152.3° (**1**) and 151.98° (**2**), are close to the empirically calculated θ values in solution, suggesting similar coordination geometries in solution and crystal states.

3.3. X-ray structure and Hirshfeld surfaces analyses

Both (**1**) and (**2**) crystallize in the monoclinic $P2_1/n$ (No. 14) space group (Table I). Their molecular structures in the crystal state are depicted in Figure 1. Selected bond lengths and angles for (**1**) and (**2**) are listed in Table II. All bond distances display typical values [71,72]. Also, the geometric parameters obtained for (**1**) resemble those observed for (**2**) (Table II).

Insert Figure 1

Insert Table II

Our X-ray crystallographic results show that each product displays a seven-coordinate metal centre in a distorted pentagonal bipyramidal coordination geometry (Figure 1 and Table II). The same coordination geometry was observed for $[(RO_2CCH_2CH_2)_2Sn(PDTC)_2]$ (R = Me, Et, Pr or Bu; PDTC = pyrrolidinodithiocarbamate) [38]. In **1** and **2**, the apical positions are occupied by similar Sn-C bonds. In addition, the C-Sn-C angles are smaller than 180°, namely 152.28(9)° for (**1**) and 151.98(12)° for (**2**). The equatorial plane of each product accommodates two bidentate morpholinodithiocarbamate ligands and one C=O···Sn interaction. The morpholinodithiocarbamate ligands are unsymmetrically bound to tin. For (**1**), the S1-Sn1, S2-Sn1, S3-Sn1 and S4-Sn1 distances amount to 2.6120(5), 2.8873(6), 2.5870(5) and 2.8655(6) Å, respectively. For (**2**), the respective distances are 2.5799(7), 2.9064(7), 2.5810(7) and 2.9179(7) Å. Furthermore, the intramolecular C=O···Sn contacts do not considerably vary in length on going from (**1**) [O1···Sn1, 2.632 Å] to (**2**) [O1···Sn1, 2.618 Å] and are more than 1.0 Å shorter than the sum of O and Sn van der Waals radii, 3.70 Å [73]. The O1···Sn1 distances observed for (**1**) and (**2**) are also shorter than those obtained for [$(RO_2CCH_2CH_2)_2Sn(PDTC)_2$] [38].

Nonclassical hydrogen bonds for (**1**) and (**2**) are listed in Table III. They were identified by Mercury [58] and PLATON [59] and confirmed by Hirshfeld surface analysis [62-65]. In addition to intramolecular C-H···S contacts, the supramolecular architecture of (**1**) comprises 1D zigzag chains along the [100] direction assembled by the C4-H4A···O3, C4-H4B···O6, C4-H4C···O6, C16-H16B···S2, and C18-H18B···S4 interactions (Figure 2). Adjacent chains are interconnected by the C2-H2A···O5 and C16-H16A···O5 contacts, establishing 2D networks parallel to the *ab* plane. The C16-H16A···O5 contacts form 1D zigzag chains along the [010] direction. In the supramolecular structure of (**1**), both O5 and O6 are involved in bifurcated hydrogen-bonding schemes. Our results also show that C4 is an excellent nonclassical hydrogen-bond donor.

Insert Table III

Insert Figure 2

According to Table III, the supramolecular arrangement of (**2**) does not involve any ring-type motif but exhibits a robust *C*(8) C-H···S supramolecular synthon. In (**2**), the C1-H1B···O3 and C9-H9B···S1 contacts form 1D chains along the diagonal of the [101] direction, while the C4-H4B···O5 interactions establish 1D chains along the *a* axis. Together, these contacts form 2D sheets parallel to the *ac* plane (Figure 3). Adjacent 2D networks are assembled along the [010] direction by 1D zigzag chains formed by the C9-H9A···S3, C12-H12A···O6 and C18-H18A···S1 interactions. In the crystal structure of (**2**), S1 is involved in bifurcated hydrogen-bonding schemes.

Insert Figure 3

According to our Hirshfeld surface analysis (Figures S3 and S4, Appendix A), isotropic van der Waals H···H contacts account for 58.2% of the Hirshfeld surface area for (**1**), while H···O/O···H close contacts correspond to 21.0%. Besides, H···S/S···H contacts contribute 14.5% to the Hirshfeld surface area for (**1**). The Hirshfeld surface analysis of (**2**) has shown that dispersive H···H contacts respond for 63.3% of its Hirshfeld surface area, whereas H···O/O···H and H···S/S···H close contacts contribute 18.0% and 14.0%, respectively.

3.4. DFT Calculations

A DFT study of the six- and seven-coordinate forms of (**1**) and (**2**) has been carried out at the B3LYP/LACV3P** level of calculation. The optimized geometries of these linkage isomers are depicted in Figure 4. Their Cartesian coordinates are listed in Table S1 (Appendix A). The geometric parameters calculated for the seven-coordinate complexes resemble those obtained by X-ray crystallography (Table S2, Appendix A). As expected, Figure 4 shows that the hexacoordinated isomers exhibit a distorted octahedral geometry, and the semi-coordinated C=O bond is slightly longer than the other C=O bond for the heptacoordinated products. For (**1**), the seven-coordinate complex is 3.8 kcal mol^{-1} more stable than the six-coordinate form. A similar energy difference (3.7 kcal mol^{-1}) was found for (**2**). These values provide an upper-bound estimate of the intramolecular C=O···Sn interaction energy: -3.7 kcal mol^{-1}. Moreover, the gas-phase enthalpy difference between the six- and seven-coordinate isomers at 298.15 K amounts to 3.5 kcal mol^{-1} for (**1**) and 3.9 kcal mol^{-1} for (**2**).

Insert Figure 4

4. Conclusions

Two diestertin(IV) morpholinodithiocarbamate complexes, (**1**) and (**2**), were synthesized and characterized by vibrational (FTIR) and multinuclear (^{1}H, ^{13}C and ^{119}Sn) NMR spectroscopy and X-ray crystallography. According to our X-ray diffraction study, both (**1**) and (**2**) display a distorted pentagonal bipyramidal coordination geometry since the apical positions are occupied by ester groups and the equatorial plane accommodates two (unsymmetrically bound) bidentate morpholinodithiocarbamate ligands and one intramolecular C=O···Sn semi-coordination. Furthermore, our supramolecular analysis revealed that the crystal packing of both products is governed by nonclassical C-H···O and C-H···S hydrogen bonds. Finally, DFT calculations at the B3LYP/LACV3P** level provided an upper-bound estimate of the C=O···Sn interaction energy, namely -3.7 kcal mol^{-1}.

Appendix A. Supplementary data

CCDC 1533978 and 1533979 contain the supplementary crystallographic data for (**1**) and (**2**), respectively. These data can be obtained free of charge via http://www.ccdc.cam.ac.uk/conts/retrieving.html, or from the Cambridge Crystallographic Data Centre, 12 Union Road, Cambridge CB2 1EZ, UK; fax: (+44) 1223-336-033; or e-mail: deposit@ccdc.cam.ac.uk. Supplementary figures and tables associated with this article can be found in the online version.

Acknowledgements

The authors are grateful to the Brazilian funding agencies CNPq (306764/2013-0), CAPES (5687-15-2), FAPEMIG (APQ 01832-14) and FAPERJ (E-26/201.338-2014) for sponsorship.

References

[1] E. Frankland, Justus Liebigs Ann. Chem. 71 (1849) 171.

[2] E. Frankland, J. Chem. Soc. 2 (1850) 297.

[3] A.G. Davies, P.J. Smith, Tin, in: G.F. Wilkinson, F.G. Stone, E.W. Abel (Eds.), Comprehensive Organometallic Chemistry, Pergamon Press, Oxford, 1982, vol. 2, pp. 523-527.

[4] M. Gielen, Coord. Chem. Rev. 151 (1996) 41.

[5] S.H.L. Thoonen, B.-J. Deelman, G. van Koten, J. Organomet. Chem. 689 (2004) 2145.

[6] A.C.A. Sousa, M.R. Pastorinho, S. Takahashi, S. Tanabe, Environ. Chem. Lett. 12 (2014) 117.

[7] R.E. Hutton, V. Oakes, Synthesis of Novel Substituted Alkyltin Halides, in: J.J. Zuckerman (Ed.), Organotin Compounds: New Chemistry and Applications, American Chemical Society, Washington DC, 1976, vol. 157, ch. 8, pp. 123-133.

[8] D. Lanigan, E.L. Weinberg, The Use of Estertin Stabilizers in PVC, in: J.J. Zuckerman (Ed.), Organotin Compounds: New Chemistry and Applications, American Chemical Society, Washington DC, 1976, vol. 157, ch. 9, pp. 134-154.

[9] A.H. Penninks, W. Seinen, Food Chem. Toxicol. 20 (1982) 909.

[10] R.E. Hutton, J.W. Burley, V. Oakes, J. Organomet. Chem. 156 (1978) 369.

[11] P.G. Harrison, T.J. King, M.A. Healy, J. Organomet. Chem. 182 (1979) 17.

[12] L. Tian, Z. Shang, Q. Yu, L. Zhang, Appl. Organomet. Chem. 19 (2005) 179.

[13] L. Tian, Q. Yu, Z. Shang, Y. Sun, L. Zhang, Appl. Organomet. Chem. 19 (2005) 677.

[14] L.-J. Tian, Y.-X. Sun, X.-J. Liu, G.-M. Yang, Z.-C. Shang, Polyhedron 24 (2005) 2027.

[15] G.M. de Lima, B.F. Milne, R.P. Pereira, A.M. Rocco, J.M.S. Skakle, A.J. Travis, J.L. Wardell, S.M.S.V. Wardell, J. Mol. Struct. 921 (2009) 244.

[16] I. Omae, Appl. Organomet. Chem. 24 (2010) 374.

[17] L.-C. Zhang, S.-L. Zheng, H. Xue, Z.-M. Zhu, W.-S. You, Y.-G. Li, E. Wang, Dalton Trans. 39 (2010) 3369.

[18] S.M. Kim, J.-H. Ju, O.-S. Jung, S.-H. Moon, K.-Y. Park, Bull. Korean Chem. Soc. 33 (2012) 2753.

[19] H. Yang, L.-C. Zhang, L. Yang, X.-L. Zhang, W.-S. You, Z.-M. Zhu, Inorg. Chem. Commun. 29 (2013) 33.

[20] J.P. Eußner, S. Dehnen, Z. Anorg. Allg. Chem. 640 (2014) 295.

[21] Q. Liu, X. Shi, C. Zhang, L. Tian, Main Group Met. Chem. 38 (2015) 93.

[22] L.-P. Ji, J. Du, J.-S. Li, L.-C. Zhang, X.-J. Sang, H. Yang, H.-J. Cui, Z.-M. Zhu, RSC Adv. 6 (2016) 28956.

[23] F. Fu, Z. Li, L. Tian, H. Pan, F. Kayser, R. Willem, M. Gielen, Bull. Soc. Chim. Belg. 101 (1992) 279.

[24] L. Tian, Z. Zhou, B. Zhao, Y. Su, C. Zhang, Main Group Met. Chem. 21 (1998) 735.

[25] L. Tian, Z. Zhou, B. Zhao, W. Yu, P. Yang, Synth. React. Inorg. Met.-Org. Chem. 30 (2000) 1363.

[26] L. Tian, B. Zhao, F. Li, Synth. React. Inorg. Met.-Org. Chem. 31 (2001) 139.

[27] L. Tian, Z. Zhou, Q. Yu, X. Liu, Synth. React. Inorg. Met.-Org. Chem. 33 (2003) 259.

[28] H.-S. Cheng, T.-L. Hwang, C.-S. Liu, J. Organomet. Chem. 254 (1983) 43.

[29] O.-S. Jung, J.H. Jeong, Y.S. Sohn, J. Organomet. Chem. 397 (1990) 17.

[30] R. Balasubramanian, Z.H. Chohan, S.M.S.V. Doidge-Harrison, R.A. Howie, J.L. Wardell, Polyhedron 16 (1997) 4283.

[31] R.A. Howie, S.M.S.V. Wardell, Acta Crystallogr., Sect. E: Struct. Rep. Online 58 (2002) m257.

[32] Y. Dong, Acta Crystallogr., Sect. E: Struct. Rep. Online 63 (2007) m2917.

[33] G.M. de Lima, S.M.S.V. Wardell, J.L. Wardell, E.R.T. Tiekink, Acta Crystallogr., Sect. E: Struct. Rep. Online 65 (2009) m1635.

[34] H. Buchanan, R.A. Howie, A. Khan, G.M. Spencer, J.L. Wardell, J.H. Aupers, J. Chem. Soc., Dalton Trans. (1996) 541.

[35] S.W. Ng, C. Wei, V.G.K. Das, J.-P. Charland, F.E. Smith, J. Organomet. Chem. 364 (1989) 343.

[36] S.W. Ng, V.G.K. Das, Acta Crystallogr., Sect. C: Cryst. Struct. Commun. 51 (1995) 2492.

[37] V.G.K. Das, N.S. Weng, P.J. Smith, Inorg. Chim. Acta 49 (1981) 149.

[38] B.P. de Morais, C.L. Donnici, B.L. Rodrigues, G.M. de Lima, J.L. Wardell, R.S. Bitzer, J. Organomet. Chem. 832 (2017) 57.

[39] C.S. Rocha, B.P. de Morais, B.L. Rodrigues, C.L. Donnici, G.M. de Lima, J.D. Ardisson, J.A. Takahashi, R.S. Bitzer, Polyhedron 117 (2016) 35.

[40] L.C. Dias, G.M. de Lima, J.A. Takahashi, J.D. Ardisson, Appl. Organomet. Chem. 29 (2015) 305.

[41] B.P. de Morais, G.M. de Lima, C.B. Pinheiro, R.A. Burrow, D.F. Back, R.A.S. San Gil, D.C. Menezes, J.D. Ardisson, Polyhedron 102 (2015) 344.

[42] B.P. de Morais, G.M. de Lima, C.B. Pinheiro, R.A.S. San Gil, J.A. Takahashi, D.C. Menezes, J.D. Ardisson, J. Mol. Struct. 1094 (2015) 246.

[43] I.P. Ferreira, G.M. de Lima, E.B. Paniago, W.R. Rocha, J.A. Takahashi, C.B. Pinheiro, J.D. Ardisson, Polyhedron 79 (2014) 161.

[44] I.P. Ferreira, G.M. de Lima, E.B. Paniago, W.R. Rocha, J.A. Takahashi, C.B. Pinheiro, J.D. Ardisson, Eur. J. Med. Chem. 58 (2012) 493.

[45] L.C. Dias, M.M.M. Rubinger, J.P. Barolli, J.D. Ardisson, I.C. Mendes, G.M. de Lima, L. Zambolim, M.R.L. Oliveira, Polyhedron 47 (2012) 30.

[46] F.T. Vieira, D.C. Menezes, G.M. de Lima, J.L. Wardell, M.E. Cortés, G.A.B. Silva, A. Vilas-Boas, J.R.S. Maia, Appl. Organomet. Chem. 22 (2008) 433.

[47] D.C. Menezes, F.T. Vieira, G.M. de Lima, J.L. Wardell, M.E. Cortés, M.P. Ferreira, M.A. Soares, A.V. Boas, Appl. Organomet. Chem. 22 (2008) 221.

[48] D.C. Menezes, G.M. de Lima, G.S. de Oliveira, A.V. Boas, A.M.A. Nascimento, F.T. Vieira, Main Group Met. Chem. 31 (2008) 21.

[49] D.C. Menezes, G.M. de Lima, A.O. Porto, M.P. Ferreira, J.D. Ardisson, R.A. Silva, Main Group Met. Chem. 30 (2007) 49.

[50] C.S. Rocha, B.P. de Morais, B.L. Rodrigues, C.L. Donnici, G.M. de Lima, J.D. Ardisson, J.A. Takahashi, R.S. Bitzer, Appl. Organomet. Chem. doi: 10.1002/aoc.3645.

[51] S.W. Ng, C. Wei, V.G.K. Das, G.B. Jameson, R.J. Butcher, J. Organomet. Chem. 365 (1989) 75.

[52] O.-S. Jung, J.H. Jeong, Y.S. Sohn, Organometallics 10 (1991) 2217.

[53] S.W. Ng, Acta Crystallogr., Sect. C: Cryst. Struct. Commun. 49 (1993) 753.

[54] Agilent, CrysAlisPro, Agilent Technologies Ltd, Yarnton, Oxfordshire, England, 2014.

[55] G.M. Sheldrick, Acta Crystallogr., Sect. A: Found. Crystallogr. 64 (2008) 112.

[56] G.M. Sheldrick, Acta Crystallogr. Sect. C. Struct. Chem. 71 (2015) 3.

[57] L.J. Farrugia, J. Appl. Crystallogr. 45 (2012) 849.

[58] C.F. Macrae, P.R. Edgington, P. McCabe, E. Pidcock, G.P. Shields, R. Taylor, M. Towler, J. van de Streek, J. Appl. Crystallogr. 39 (2006) 453.

[59] (a) A.L. Spek, J. Appl. Crystallogr. 36 (2003) 7; (b) A.L. Spek, Acta Crystallogr. Sect. D. Biol. Crystallogr. 65 (2009) 148.

[60] F.H. Allen, O. Johnson, G.P. Shields, B.R. Smith, M. Towler, J. Appl. Crystallogr. 37 (2004) 335.

[61] R.H. Blessing, Acta Crystallogr., Sect. A: Found. Crystallogr. 51 (1995) 33.

[62] M.A. Spackman, J.J. McKinnon, CrystEngComm 4 (2002) 378.

[63] J.J. McKinnon, M.A. Spackman, A.S. Mitchell, Acta Crystallogr. Sect. B Struct. Sci. 60 (2004) 627.

[64] J.J. McKinnon, D. Jayatilaka, M.A. Spackman, Chem. Commun. (2007) 3814.

[65] M.A. Spackman, D. Jayatilaka, CrystEngComm 11 (2009) 19.

[66] S.K. Wolff, D.J. Grimwood, J.J. McKinnon, M.J. Turner, D. Jayatilaka, M.A. Spackman, CrystalExplorer (Version 3.1), University of Western Australia, 2012.

[67] JAGUAR (Version 7.9), Schrödinger, LLC, New York, NY (2011).

[68] A.D. Becke, J. Chem. Phys. 98 (1993) 5648.

[69] (a) D. Dakternieks, H. Zhu, D. Masi, C. Mealli, Inorg. Chem. 31 (1992) 3601; (b) A.N. Gupta, V. Kumar, V. Singh, A. Rajput, L.B. Prasad, M.G.B. Drew, N. Singh, J. Organomet. Chem. 787 (2015) 65.

[70] (a) J. Holecek, M. Nadvornik, K. Handlir, A. Lycka, *J. Organomet. Chem.* **1986**, *315*, 299. (b) T. P. Lockhart, W. F. Manders, J. J. Zuckerman, *J. Am. Chem. Soc.* **1985**, *107*, 4546. (c) T. P. Lockhart, W. F. Manders, *J. Am. Chem. Soc.* **1987**, *109*, 7015.

[71] F.H. Allen, O. Kennard, D.G. Watson, L. Brammer, A.G. Orpen, R. Taylor, J. Chem. Soc., Perkin Trans. 2 (1987) S1.

[72] A.G. Orpen, L. Brammer, F.H. Allen, O. Kennard, D.G. Watson, R. Taylor, J. Chem. Soc., Dalton Trans. (1989) S1.

[73] A. Bondi, J. Phys. Chem. 68 (1964) 441.

[74] (a) M.C. Etter, Acc. Chem. Res. 23 (1990) 120; (b) M.C. Etter, J.C. MacDonald, J. Bernstein, Acta Crystallogr., Sect. B: Struct. Sci. 46 (1990) 256.

Captions for Schemes, Figures and Tables

Table I. Crystal data and structure refinement parameters for $[(RO_2CCH_2CH_2)_2Sn(MDTC)_2]$ (R = Me (**1**) or Et (**2**); MDTC = morpholinodithiocarbamate).

Table II. Selected bond lengths (Å) and angles (°) for (**1**) and (**2**).

Table III. Noncovalent interactions and supramolecular motifs for (**1**) and (**2**).[a]

Scheme 1. Preparation of $[(RO_2CCH_2CH_2)_2Sn(MDTC)_2]$ (R = Me (**1**) or Et (**2**); MDTC = morpholinodithiocarbamate).

Scheme 2. Atom numbering scheme for ^{1}H and $^{13}C\{^{1}H\}$ NMR assignments.

Figure 1. Atom numbering schemes and molecular structures of complexes (**1**) (left) and (**2**) (right) in the crystal state. Ellipsoids are drawn at the 50% probability level and hydrogen atoms are omitted for clarity.

Figure 2. Packing diagram of (**1**) highlighting a 1D zigzag chain along the [100] direction. H atoms except those involved in hydrogen bonds are omitted for clarity. Symmetry codes: (*ii*) -x,-y,2-z; (*iii*) -1+x,y,z; (*iv*) 1-x,-y,2-z; (*vi*) 1+x,y,z.

Figure 3. Packing diagram of (**2**) showing a 2D network parallel to the [101] plane. H atoms except those involved in hydrogen bonds are omitted for clarity. Symmetry codes: (*vi*) 1+x,y,z; (*vii*) -0.5+x,0.5-y; (*ix*) 0.5+x,0.5-y,0.5+z.

Figure 4. DFT-optimized geometries of the six- (left) and seven-coordinate (right) isomers of (**1**) (top) and (**2**) (bottom). H atoms are omitted for clarity. Bond distances are given in Å.

Table I

	(**1**)	(**2**)
Crystal description	Colourless prism	Colourless prism
Empirical formula	$C_{18}H_{30}N_2O_6S_4Sn$	$C_{20}H_{34}N_2O_6S_4Sn$
M/g mol^{-1}	617.37	645.42
T/K	150(1)	150(1)
λ/Å	0.71073 (Mo-Kα)	0.71073 (Mo-Kα)
Crystal system	Monoclinic	Monoclinic
Space group	$P2_1/n$ (No. 14)	$P2_1/n$ (No. 14)
a/Å	11.2490(2)	12.8474(5)
b/Å	17.1944(2)	16.1777(6)
c/Å	13.0525(2)	13.6492(6)
β/°	99.606(2)	106.594(4)
V/Å^3	2489.21(7)	2718.7(2)
Z	4	4
D_x/Mg m^{-3}	1.647	1.577
μ/mm^{-1}	1.398	1.283
F(000)	1256	1320
Crystal size/mm^3	0.1 x 0.1 x 0.1	0.1 x 0.1 x 0.1
θ range/°	1.98 to 29.48	1.92 to 29.56
Index ranges	$-15 \le h \le 15$ $-22 \le k \le 22$ $-16 \le l \le 17$	$-17 \le h \le 16$ $-21 \le k \le 16$ $-18 \le l \le 17$
Reflections collected	57968	13920
Independent reflections	6520	6513
Observed reflections	5637 [$I > 2\sigma(I)$]	5178 [$I > 2\sigma(I)$]
Completeness to θ_{max}	100%	100%
Absorption correction	Multi-scan [61]	Multi-scan [61]
T_{max} and T_{min}	1.0000 and 0.7984	1.0000 and 0.7233
Refinement method	Full-matrix least-squares on F^2	Full-matrix least-squares on F^2
Data / restraints / parameters	6520 / 0 / 280	6513 / 0 / 298
Goodness-of-fit on F^2	1.044	1.093
Final R indices [$I > 2\sigma(I)$][a]	$R_1 = 0.0255$, $wR_2 = 0.0550$	$R_1 = 0.0301$, $wR_2 = 0.0686$
R indices (all data)[a]	$R_1 = 0.0334$, $wR_2 = 0.0594$	$R_1 = 0.0479$, $wR_2 = 0.0846$
$\Delta\rho_{max}$ and $\Delta\rho_{min}$/e Å^{-3}	1.004 and -0.449	0.688 and -0.658
Deposition number	CCDC 1533978	CCDC 1533979

[a] $R_1 = (\Sigma_{hkl} ||F_o| - |F_c||)/(\Sigma_{hkl} |F_o|)$ and $wR_2 = \{[\Sigma_{hkl} w(F_o^2 - F_c^2)^2]/[\Sigma_{hkl} w(F_o^2)^2]\}^{½}$.

Table II.

(**1**)		(**2**)	
C1-Sn1 2.134(2)	C1-Sn1-C5 152.28(9)	C1-Sn1 2.134(3)	S2-C11-S1 118.58(15)
C5-Sn1 2.138(2)	S1-Sn1-S2 64.690(15)	C6-Sn1 2.138(2)	S4-C16-S3 118.32(15)
S1-Sn1 2.6120(5)	S3-Sn1-S4 65.370(15)	S1-Sn1 2.5799(7)	C1-Sn1-C6 151.98(12)
S2-Sn1 2.8873(6)	O1-Sn1-S2 76.34(4)	S2-Sn1 2.9064(7)	S3-Sn1-S4 64.46(2)
S3-Sn1 2.5870(5)	O1-Sn1-S4 74.08(4)	S3-Sn1 2.5810(7)	S1-Sn1-S2 64.83(2)
S4-Sn1 2.8655(6)	S2-C9-S1 118.48(12)	S4-Sn1 2.9179(7)	O1-Sn1-S2 79.78(5)
O1-Sn1 2.632 (2)	S4-C14-S3 118.23(12)	O1-Sn1 2.618(2)	O1-Sn1-S4 73.43(5)
C9-S1 1.732(2)		C11-S1 1.729(3)	
C9-S2 1.702(2)		C11-S2 1.707(3)	
C14-S3 1.737(2)		C16-S3 1.739(3)	
C14-S4 1.705(2)		C16-S4 1.693(3)	
C9-N1 1.336(3)		C16-N2 1.338(3)	
C14-N2 1.329(3)		C11-N1 1.336(3)	
C3-O1 1.201(2)		C8-O3 1.200(3)	
C3-O2 1.327(3)		C8-O4 1.343(3)	
C7-O3 1.203(3)		C3-O1 1.215(3)	
C7-O4 1.331(3)		C3-O2 1.323(4)	

Table III.

Type	Geometric parameters				Motif[b]
D–H···A	D–H/Å	H···A/Å	D···A/Å	D–H···A/°	$G^{a}_{d}(r)$
(**1**)					
C2-H2A···O5*i*	0.97	2.65	3.450(3)	139.6	$R^{2}_{2}(20)$
C4-H4A···O3*ii*	0.96	2.63	3.487(3)	148.3	$R^{2}_{2}(20)$
C4-H4B···O6*iii*	0.96	2.54	3.377(3)	145.7	*C*(12)
C4-H4C···O6*iv*	0.96	2.50	3.432(3)	163.7	$R^{2}_{2}(24)$
C10-H10B···S1	0.97	2.54	3.040(2)	111.9	*S*(5)
C12-H12A···S2	0.97	2.52	3.034(2)	113.3	*S*(5)
C15-H15B···S3	0.97	2.53	3.052(2)	113.6	*S*(5)
C16-H16A···O5*v*	0.97	2.52	3.468(3)	165.1	*C*(13)
C16-H16B···S2*vi*	0.97	2.77	3.609(2)	145.3	*C*(8)
C17-H17A···S4	0.97	2.52	3.042(2)	113.5	*S*(5)
C18-H18B···S4*iv*	0.97	2.96	3.466(2)	113.8	$R^{2}_{2}(12)$
(**2**)					
C1-H1B···O3*vii*	0.97	2.66	3.593	162.4	*C*(7)
C4-H4B···O5*vi*	0.97	2.42	3.308(4)	151.8	*C*(12)
C5-H5C···O1	0.96	2.62	3.115(5)	112.4	*S*(6)
C9-H9A···S3*viii*	0.97	2.95	3.647(3)	129.4	*C*(8)
C9-H9B···S1*ix*	0.97	3.02	3.763(3)	134.3	*C*(8)
C12-H12A···O6*viii*	0.97	2.41	3.301(4)	152.1	*C*(12)
C12-H12B···S1	0.97	2.50	2.994(3)	111.3	*S*(5)
C14-H14A···S2	0.97	2.56	3.038(3)	110.4	*S*(5)
C17-H17A···S3	0.97	2.50	3.017(3)	113.2	*S*(5)
C18-H18A···S1*x*	0.97	3.02	3.907(3)	152.3	*C*(8)
C19-H19B···S4	0.97	2.56	3.076(3)	113.4	*S*(5)

[a] Symmetry codes: (*i*) -x,1-y,2-z; (*ii*) -x,-y,2-z; (*iii*) -1+x,y,z; (*iv*) 1-x,-y,2-z; (*v*) 0.5-x,-0.5+y,1.5-z; (*vi*) 1+x,y,z; (*vii*) -0.5+x,0.5-y,-0.5+z; (*viii*) 0.5-x,0.5+y,2.5-z; (*ix*) 0.5+x,0.5-y,0.5+z; (*x*) 0.5-x,-0.5+y,2.5-z.

[b] Etter's graph-set assignment [74].

Scheme 1

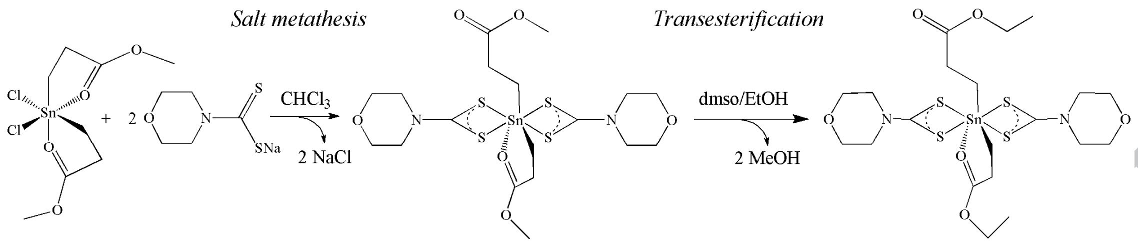

(**1**) (**2**)

Scheme 2

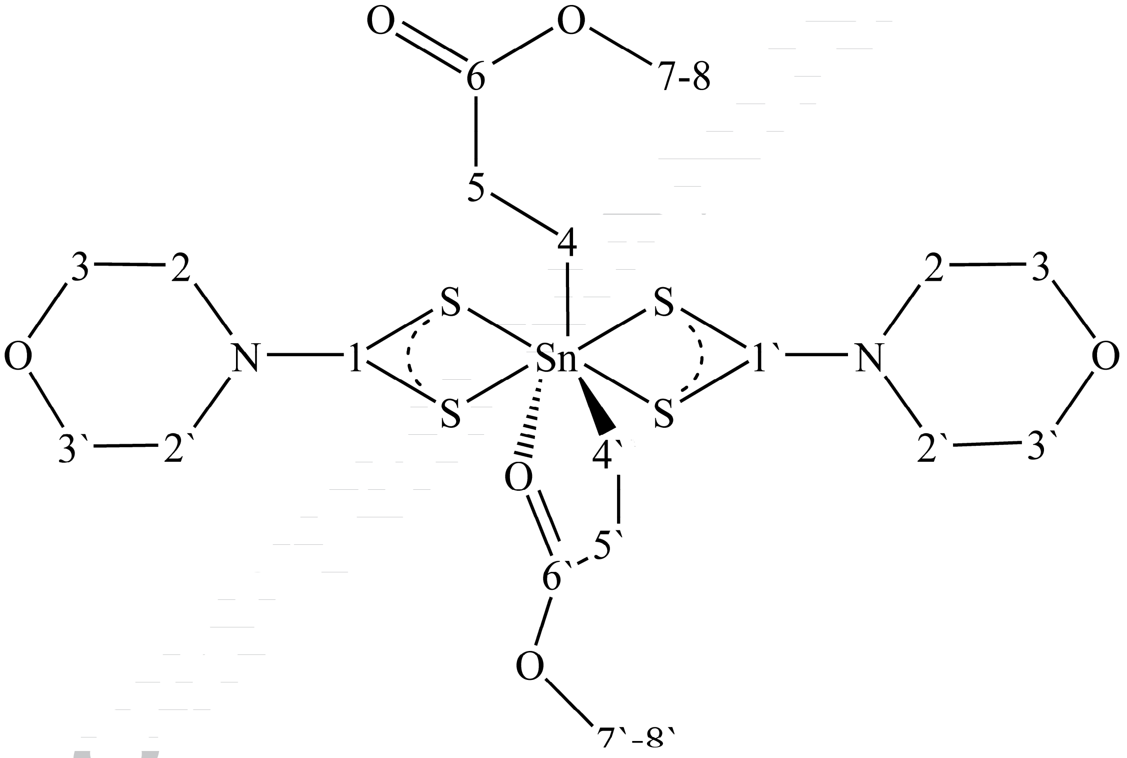

Figure 1

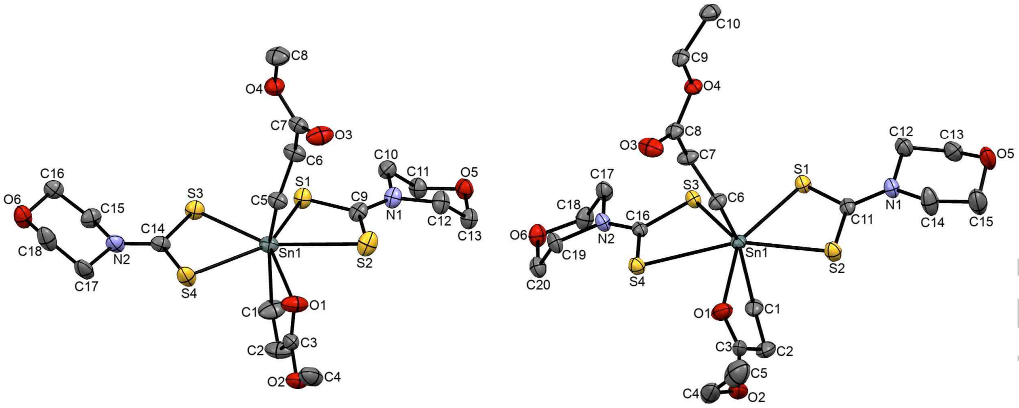
C8
O4
C7
O3
C6
C16
O6
C15
C14
S3
C5
S1
C9
C10
C11
O5
N1
C12
C13
C18
N2
Sn1
S2
C17
S4
C1
O1
C2
C3
O2
C4
C10
C9
O4
O3
C8
C7
C12
C13
O5
C17
S3
C6
S1
C18
N1
C16
C11
O6
N2
C14
C15
C19
Sn1
S4
S2
C20
O1
C1
C3
C2
C5
C4
O2

Figure 2

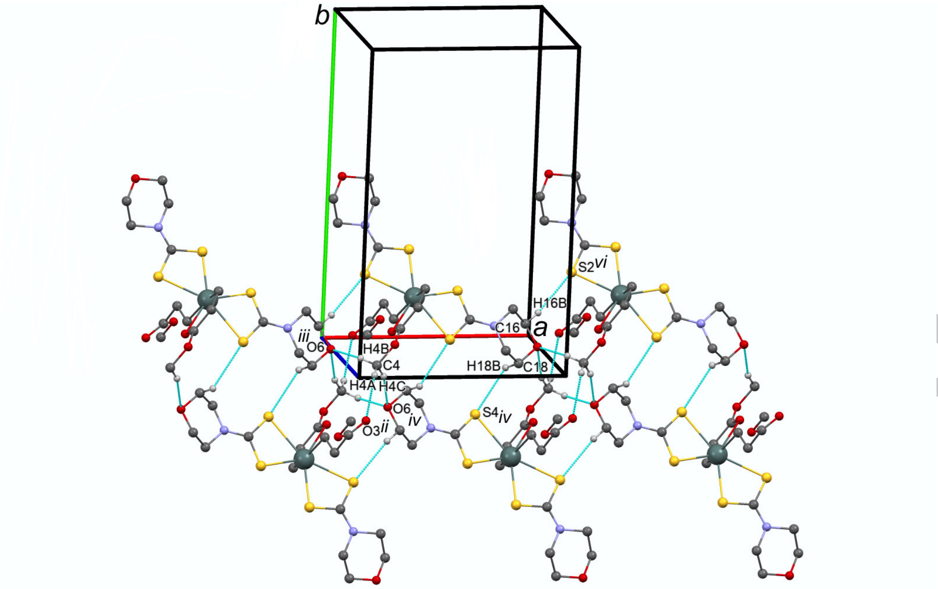

Figure 3

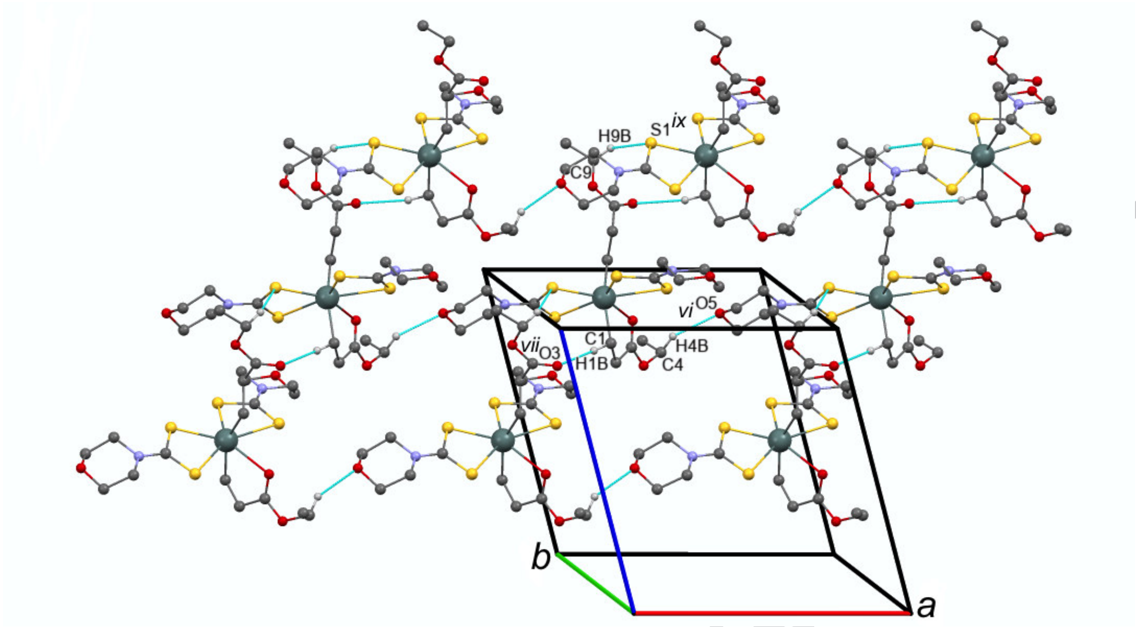

Figure 4

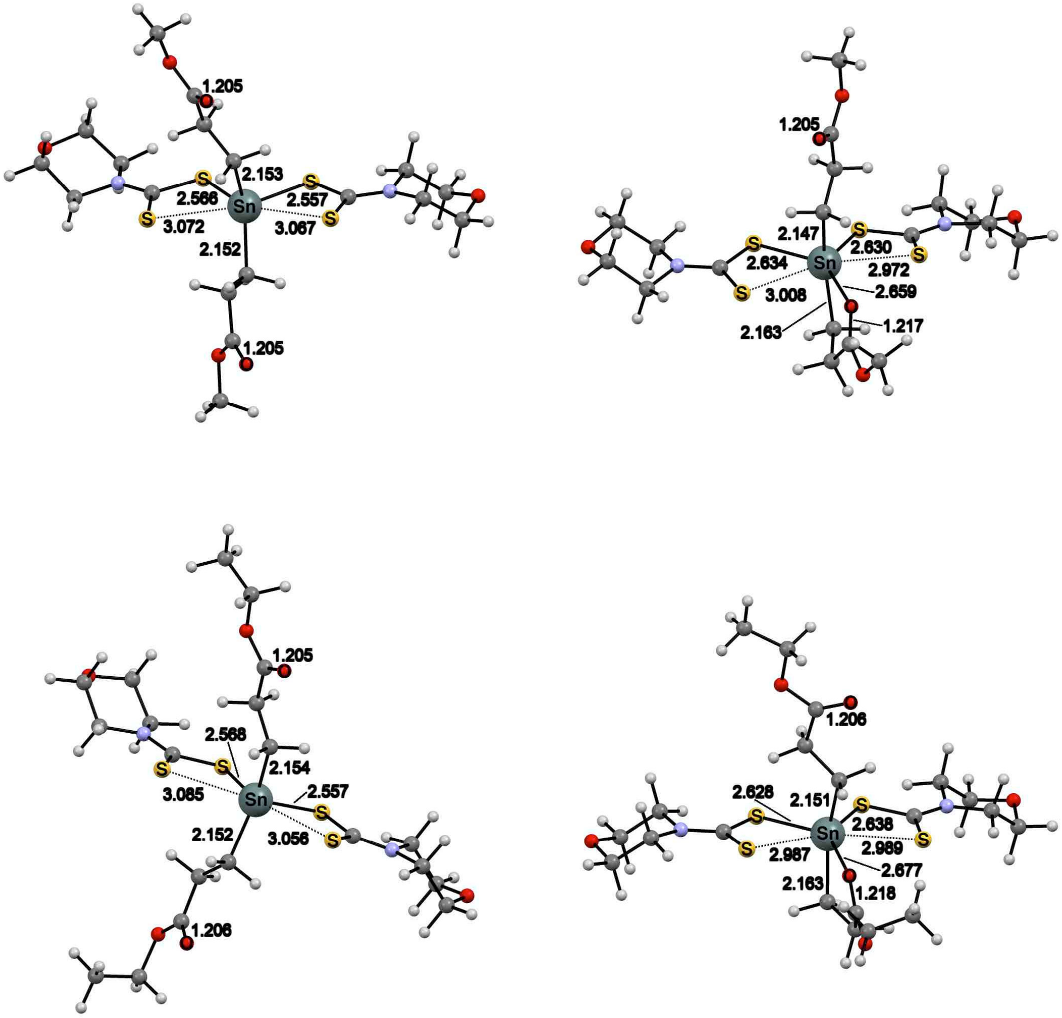
1.205
2.153
2.566
2.557
Sn
3.072
3.067
2.152
1.205
1.205
2.147
2.630
2.634
Sn
2.972
3.008
2.659
2.163
1.217
1.205
2.568
2.154
2.557
3.085
Sn
2.152
3.056
1.206
1.206
2.628
2.151
2.638
Sn
2.989
2.967
2.677
2.163
1.218

The diestertin(IV) dithiocarbamate complexes [$(RO_2CCH_2CH_2)_2Sn(MDTC)_2$] (R = Me (**1**) or Et (**2**); MDTC = morpholinodithiocarbamate) have been prepared, characterized and structurally authenticated. Complex (**1**) has been obtained from the reaction of [$(MeO_2CCH_2CH_2)_2SnCl_2$] with sodium morpholinodithiocarbamate (NaMDTC) in $CHCl_3$, and its transesterification reaction with EtOH in the presence of dmso yielded complex (**2**).

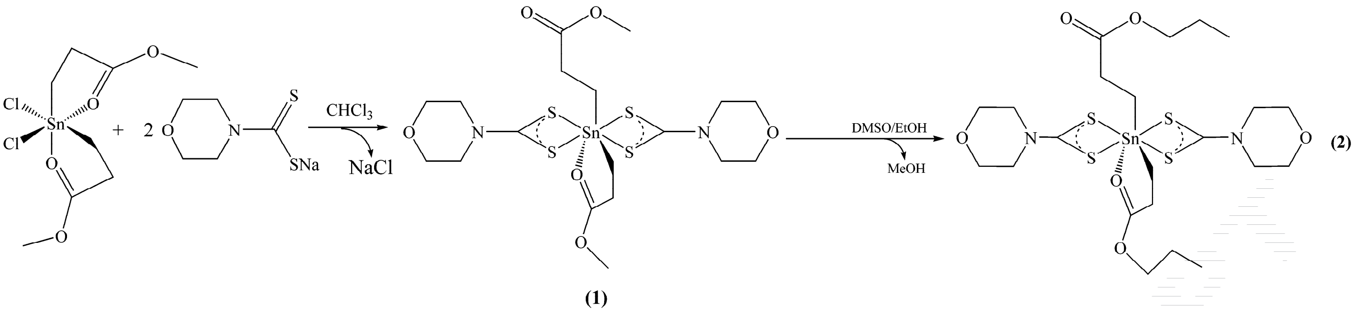
Cl
Cl
Sn
O
O
+ 2
S
SNa
N
CHCl3
NaCl
S
Sn
(1)
DMSO/EtOH
MeOH
(2)

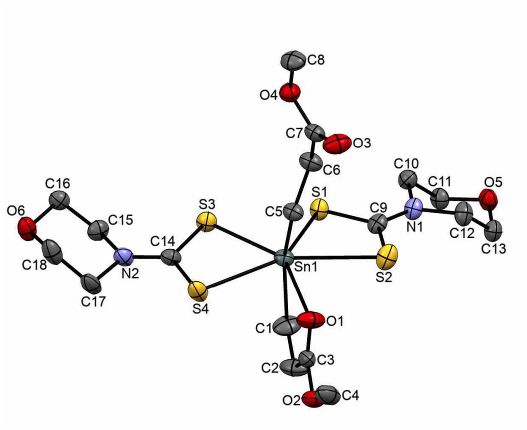
C8
O4
C7
O3
C6
C5
S1
C9
N1
C10
C11
O5
C12
C13
S2
Sn1
S3
C14
N2
C15
C16
O6
C18
C17
S4
C1
O1
C2
C3
O2
C4

(1)

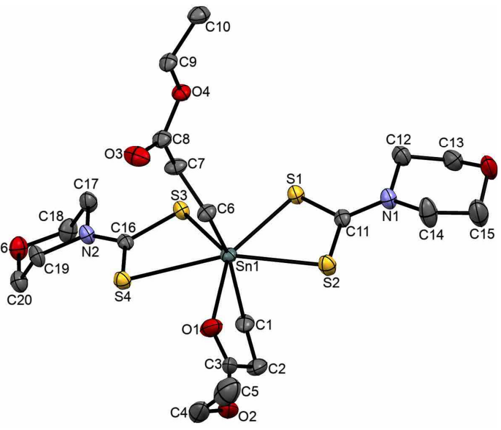
C10
C9
O4
C8
O3
C7
C6
S3
C17
C18
N2
C16
O6
C19
C20
S4
Sn1
S1
C11
N1
C12
C13
C14
C15
S2
O1
C1
C2
C3
C5
C4
O2

(2)